Analyst

ROYAL SOCIETY OF CHEMISTRY

PAPER

View Article Online
View Journal | View Issue

Published on 09 December 2020. Downloaded by University of Prince Edward Island on 5/15/2021 6:49:00 AM.

Check for updates

Cite this: *Analyst*, 2021, **146**, 1295

A novel signal amplified electrochemiluminescence biosensor based on MIL-53(Al)@CdS QDs and SiO_2@AuNPs for trichlorfon detection

Defen Feng,†[a] Fucun Wei,†[a] Yeyu Wu,*[a] Xuecai Tan,*[a] Fang Li,[a] Yongkuai Lu,[a] Gaochao Fan[b] and Heyou Han[c]

Received 31st October 2020,
Accepted 2nd December 2020

DOI: 10.1039/d0an02158j

rsc.li/analyst

An ultrasensitive electrochemiluminescence (ECL) biosensor was developed based on MIL-53(Al)@CdS QDs and SiO_2@AuNPs for trichlorfon detection. Metal–organic frameworks (MOFs) were used as a loading platform that provided a large surface area to load targets and modified materials onto the electrode. At the same time, SiO_2@AuNPs loaded plenty of AuNPs which effectively increased the ECL resonance energy transfer between the CdS QDs, so that the ECL signal was strongly quenched and resulted in an amplified response. In the range of 10^{-11}–10^{-4} M, the ECL response showed a linear relationship with the concentration (logarithm) of trichlorfon, and the detection limit was 5.1×10^{-12} M (S/N = 3). When the biosensor was applied to detect trichlorfon in lettuce, broccoli, cucumber, and chives, the recoveries obtained from the spiked samples were 97%–105%, 102%–104%, 100%–104%, and 98%–104%, respectively. Thus, this novel ECL biosensor has potential applications for the analysis of trichlorfon in food samples.

1 Introduction

Organophosphorus pesticides (OPs) are highly toxic and potentially carcinogenic and are widely used to protect fruits, vegetables, and crops from damage. Trichlorfon, also called dipterex, is a common OP and an effective cholinesterase inhibitor. However, the nervous system of human beings can be overstimulated by trichlorfon and serious problems can be induced such as poisoning, tumors, nausea, or even death.[1,2] In recent years, some methods have been reported for trichlorfon detection, including high-performance liquid chromatography (HPLC),[3] gas chromatography (GC),[4] capillary electrophoresis (CE)[5] and electrochemical methods.[6,7] But these methods exhibit some shortcomings, including having a narrow linear range and low sensitivity, requiring tedious preprocessing, and being time-consuming, which restrict their practical applications. So it is imperative to develop a simple, rapid, and efficient method to detect trichlorfon.

Electrochemiluminescence (ECL) is a mature and vibrant method that inherits the advantages of chemiluminescence and electrochemistry. ECL draws great attention due to its obvious merits, such as high sensitivity, rapid response, low background, and good controllability.[8] However, the low response of ECL is not conducive to detect trace substances, so it is a good choice to develop an ECL sensor with a signal amplification strategy to solve this problem. At present, several signal amplification strategies have been applied to fabricate ECL sensors, such as probes with good conductivity,[9] self-catalyzed nanocomposites,[10] ECL resonance energy transfer (ERET),[11] DNA walker,[12] and hybridization chain reaction (HCR).[13]

Among these strategies, ERET is a method that control the distance between donors and acceptors to detect the targets.[14] Generally, metal nanoparticles (*e.g.* AuNPs), rhodamine, or neutral red often acted as energy acceptors in ECL systems, especially, AuNPs which are most widely used owing to their broad absorption spectra, high extinction coefficient and strong surface plasmon resonance (SPR).[15] The energy donors

[a]*School of Chemistry and Chemical Engineering, Guangxi Key Laboratory of Chemistry and Engineering of Forest Products, Guangxi Collaborative Innovation Center for Chemistry and Engineering of Forest Products, Key Laboratory of Guangxi Colleges and Universities for Food Safety and Pharmaceutical Analytical Chemistry, Guangxi University for Nationalities, Nanning, 530006, China.*
E-mail: gxunxctan@126.com, eveyeyu@163.com
[b]*Key Laboratory of Optic-electric Sensing and Analytical Chemistry for Life Science, MOE, Shandong Key Laboratory of Biochemical Analysis, College of Chemistry and Molecular Engineering, Qingdao University of Science and Technology, Qingdao, 266042, China*
[c]*State Key Laboratory of Agricultural Microbiology, College of Science, College of Food Science and Technology, Huazhong Agricultural University, Wuhan, 430070, China*
†These authors contributed equally to this work.

Published on 09 December 2020. Downloaded by University of Prince Edward Island on 5/15/2021 6:49:00 AM.

include quantum dots (QDs), acridine orange, fluorescein, and so on. Over the past decade, QDs have proved to be promising ECL emitters, better than traditional luminescent reagents (such as bipyridylium, luminol, *etc.*), because of their advantages such as broad excitation, biocompatibility and tunable emission wavelength.[16]

Metal–organic frameworks (MOFs) are a novel class of porous materials formed primarily by the self-assembly of metal coordination centers and organic ligands.[17] Due to their uniform nanopores, excellent chemical stability, and large specific surface area, MOFs have been widely applied in the fields of sensing, gas storage, catalysis, drug delivery, and adsorption.[18] To date, just a few MOFs exhibit the property of luminescence; but the good conductivity and large surface area of MOFs make them a promising loading platform for the modification of materials of the electrode.

In this study, we report an ECL signal amplification strategy for trichlorfon detection based on a MIL-53(Al)@CdS-PEI and SiO_2@AuNP modified electrode. MIL-53(Al)@CdS QDs were used as an ECL emitter to modify the glassy carbon electrode (GCE) to attach the complementary strand (CS) of the trichlorfon aptamer. Then, the SiO_2@AuNPs were modified on the electrode by the base pairing of the labeled trichlorfon aptamer and CS, so that ERET can take place between the SiO_2@AuNPs and CdS QDs, and induce a remarkable decrease of the intensity of the ECL biosensor. During the detection of trichlorfon, trichlorfon would combine with the aptamer, and the aptamer-SiO_2@AuNPs would detach from the electrode, and then the intensity of the ECL biosensor would be restored. The change in the ECL intensity (ΔI) was correlated with the concentration for trichlorfon detection. This ECL biosensor displayed a wide linear range, low detection limit, and high specificity. This work would provide a potential method of trichlorfon detection in vegetable samples.

2 Experimental section

2.1 Materials and reagents

Thioglycolic acid (TGA) and tris(2-carboxyethyl)-phosphine hydrochloride (TCEP) were purchased from Sigma-Aldrich (Madrid, Spain). Terephthalic acid (H_2BDC), aluminum nitrate nonahydrate ($Al(NO_3)_3{\cdot}9H_2O$), chloroauric acid ($HAuCl_4$), 1-ethyl-3-(3-(dimethylamino)propyl) carbodiimide (EDC), *n*-hydroxysuccinimide (NHS), sodium sulfide ($Na_2S{\cdot}9H_2O$), polyethylenimine (PEI, W. M. 1800, 99 wt%), potassium persulfate ($K_2S_2O_8$), cadmium chloride ($CdCl_2{\cdot}2.5H_2O$), poly(dimethyldiallylammonium) chloride (PDDA, M_w 200 000–350 000, 20 wt%) and silicon dioxide (SiO_2 NPs, 99.5%, 30 nm) were purchased from Aladdin (Shanghai, China). Bovine serum albumin (BSA) was purchased from Solarbio Science & Technology Co., Ltd (Beijing, China). Trichlorfon standard was obtained from AccuStandard (New Haven, USA). Phosphate buffered saline (PBS, pH 7.4) was used to wash the electrode and prepare aptamer solutions. All the reagents were of analytical grade unless stated otherwise. The oligonucleotides used in this paper were obtained from Sangon Biotechnology Inc. (Shanghai, China).

Aptamer for trichlorfon: 5′-CGC ATC GAG AGT CGG AAA AGG CTA GTT CTT AGC GAC GTC CGA TAT TTC GTT CGA A-SH-3′.

Complementary strand (CS): 5′-COOH-(CH_2)6-TGA GTG GTT GTT CGA ACG AA-3′.

2.2 Apparatus

ECL was carried out on an MPI-B multi-parameter electrochemiluminescence system (Xi'an Remax Electronic Science & Technology Co. Ltd, China), the voltage of the photomultiplier tube (PMT) was set at 800 V, and the scanning range of potential was from −1.2 to 0 V. Cyclic voltammetry (CV) and electrochemical impedance spectroscopy (EIS) were carried out on a PGSTAT128N Autolab potentiostat/galvanostat (The Netherlands). A three-electrode system consisting of a working electrode (glassy carbon electrode, GCE, 3.0 mm in diameter), a reference electrode (Ag/AgCl and sat. KCl), and a counter electrode (platinum pole) was used throughout the detection. Fluorescence spectra (FL) were recorded using a FL-4600 fluorescence spectrometer (Hitachi, Japan). UV-visible (UV-vis) spectra were recorded using a UV-vis spectrophotometer (Agilent Cary 60, Agilent Technology, USA). Scanning electron microscopy (SEM) was performed using a SUPPRA 55 Sapphire (Carl Zeiss, Germany) and transmission electron microscopy (TEM) was performed using a Tecnai F30 (FEI, USA) and they were utilized to characterize the morphology of the materials. X-ray powder diffraction pattern (XRD) was measured using a Rigaku MiniFlex 600 X-ray diffractometer with Cu Kα radiation (λ = 1.5406 Å) at 40 kV, 40 mA. Fourier transform infrared spectra (FTIR) were measured using a Fourier transform infrared spectrometer (Nicolet iS10, Thermo Fisher Scientific, USA). Deionized water was obtained from a Milli-Q water purification system (Millipore, USA).

2.3 Preparation of MIL-53(Al)@CdS-PEI and SiO_2@AuNPs-aptamer

The synthesis of MIL-53(Al) was according to the literature,[19] and the preparation of MPA-capped CdS QDs and MIL-53(Al)@CdS-PEI was according to a previous method.[11]

AuNPs were synthesized according to the literature,[11] and the obtained AuNP solution was 0.20 mg mL^{-1}. Then, 10 mg SiO_2 nanoparticles were ultrasonically dispersed into 3 mL 5 wt% PDDA solution and shaken for 3 h at room temperature. Subsequently, the nanoparticles were centrifuged (12 000 rpm, 10 min) and washed with ultrapure water to remove unadsorbed PDDA. Next, the modified SiO_2 nanoparticles were mixed with 3 mL H_2O and AuNP solution (7–11 mL); this mixture was shaken for 2 h (room temperature). The obtained mixture was finally centrifuged and washed with water to remove unadsorbed AuNPs, and then the SiO_2@AuNP solution was collected.

For the preparation of SiO_2@AuNPs-aptamer,[20] firstly, 100 μL of 10 mM TCEP was used to activate the sulfhydryl groups of the aptamer (1 mL, 2 μM) at room temperature, and

 This journal is © The Royal Society of Chemistry 2021

Published on 09 December 2020. Downloaded by University of Prince Edward Island on 5/15/2021 6:49:00 AM.

after 1 h, SiO_2@AuNPs were added and shaken for 12 h. Subsequently, the suspension was centrifuged in an ultrafiltration tube (100 KD, 10 min, 1000 rpm) and washed with PBS (0.1 M) to remove the unbonded aptamers. Finally, the collected SiO_2@AuNPs-aptamer was dispersed in PBS (pH 7.4, 1 mL) solution and stored at 4 °C.

2.4 Fabrication and detection process of the ECL aptasensor

Before modification, the bare GCE was successively polished with 1.0, 0.3, and 0.05 μm Al_2O_3 slurry, and then was cleaned and sonicated in 1 : 1 nitric acid and ethanol, and washed with water. Subsequently, MIL-53(Al)@CdS-PEI (5 mg mL^{-1}, 2–6 μL) was modified onto the surface of the GCE and dried at room temperature. Next, at room temperature, a 600 μL mixture of EDC (20 mM) and NHS (10 mM) was added into CS solution (400 μL, 5 μM) to activate the carboxyl groups for 2 h. Then, activated CS (20 μL) was dropped onto the modified electrode and incubated overnight at 4 °C. After rinsing with PBS to remove the unconnected CS, the modified electrode was incubated with BSA (10 μL, 1%) for 2 h at room temperature to block the unbound active site and successively rinsed with PBS. After that, the modified electrode was incubated with SiO_2@AuNPs-aptamer (6–10 μL) for 1 h, and then rinsed with PBS. Finally, the aptasensor was successfully fabricated.

For trichlorfon detection (room temperature), different concentrations of trichlorfon (20 μL) were used to incubate the aptasensor for 1 h, and then PBS solution was used to rinse the electrode. Then, an ECL apparatus was used to monitor the ECL intensity of the aptasensor, while the electrode was placed in PBS solution (0.1 M, pH 7.4) containing 0.01 M $K_2S_2O_8$. The ECL aptasensor was kept at 4 °C when not in use.

2.5 Sample preparation

The vegetable samples (lettuce, broccoli, cucumber, and chives) were purchased from the local supermarket and were pretreated according to the literature with a slight modification.[21] Firstly, 2.0 g of the mashed vegetable sample was added into a 100 mL beaker and stewed for 1 h. Secondly, 10 mL H_2O was added into the mixture, sonicated for 30 min and then centrifuged, and the supernatant was collected. The abovementioned steps were repeated three times, and the supernatants were collected and filtered using a 0.22 μm PTFE membrane and transferred to a 100 mL volumetric flask. For the spiking experiment, 1.0 mL of 10^{-4} M trichlorfon was added into the sample after weighing, and then treated by the same procedures.

3 Results and discussion

3.1 Characterization of the synthesized materials

As shown in Fig. 1A, MIL-53 (Al) was a block structure with length less than 6 μm. In Fig. 1B, the AuNPs are shown as spherical dots with a diameter of 6–8 nm. The SEM image of SiO_2@AuNPs (Fig. 1C) showed that AuNPs were evenly distributed on the surface of SiO_2 to form SiO_2@AuNPs. The TEM results indicated that the CdS QD particles were smaller than 10 nm (Fig. 1D). The SEM images of the prepared CdS-PEI (Fig. 1E) and MIL-53(Al)@CdS-PEI (Fig. 1F) showed that CdS QDs and PEI, and CdS-PEI and MIL-53(Al) bonded well with each other, respectively.

FTIR characterization illustrated the bonding performance of MIL-53(Al)@CdTe-PEI. As shown in Fig. 2A, compared to

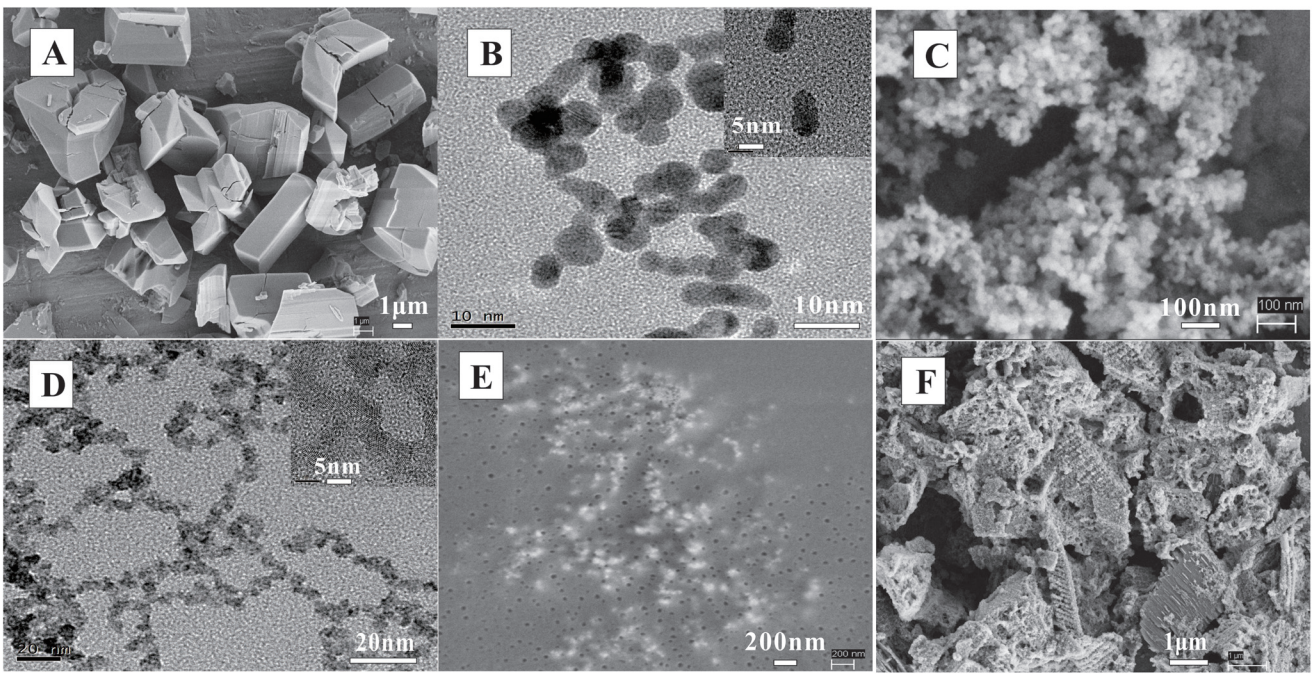

Fig. 1 SEM images and TEM images of (A) MIL-53(Al), (B) AuNPs, (C) SiO_2@AuNPs, (D) CdS QDs, (E) CdS QDs-PEI and (F) MIL-53(Al)@CdS-PEI.

Published on 09 December 2020. Downloaded by University of Prince Edward Island on 5/15/2021 6:49:00 AM.

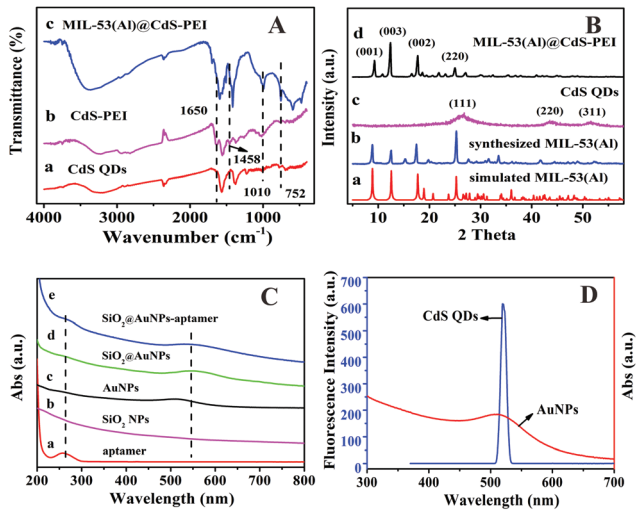

Fig. 2 (A) FTIR spectra, (B) powder X-ray diffraction pattern, (C) UV-vis spectrum, and (D) fluorescence emission spectrum of the synthesized materials.

CdS QDs (curve a), the FTIR spectra of CdS-PEI (curve b) exhibited characteristic peaks at 1010, 1458, and 1650 cm^{-1}, which corresponded to the $-NH_2$ rocking of the amide bond, C–N stretching and C=O stretching, respectively. The characteristic peak of the MIL-53(Al)@CdS-PEI composite (curve c) at 752 cm^{-1} corresponded to the Al–O absorption vibration of MIL-53(Al) and contained the characteristic peaks of CdS-PEI, which indicated the successful synthesis of MIL-53(Al)@CdS-PEI.

According to the XRD patterns (Fig. 2B), the pattern of MIL-53(Al) almost corresponded to its simulated curve (curve a), and the identical peaks at 2θ = 8.8°, 12.5°, 17.7°, and 25.3°, which represented (001), (003), (002) and (220) crystal planes, respectively, indicated the successful synthesis. The XRD pattern of the as-prepared CdS QDs showed peaks at 2θ = 28°, 43°, and 51°, which represented the planes of (110), (220) and (311), respectively. The pattern of MIL-53(Al)@CdS-PEI almost agreed with the MIL-53(Al) one (curve a), but the intensity of the characteristic peak of CdS was weak because the amount of CdS in the composite was small.

According to the UV-vis characterization (Fig. 2C), the distinct absorption at 260 nm of the aptamer was related to the characteristic absorption of adenine and thymine bases of DNA. SiO_2 did not exhibit an obvious absorption peak and the AuNPs exhibited an absorption peak at 515 nm. For SiO_2@AuNPs, the absorption peak of AuNPs was slightly red-shifted to 525 nm indicating that AuNPs were successfully bound with NH_2 grafted on SiO_2. This phenomenon of red-shift could be attributed to the increase in the local refractive index of AuNPs, which surrounded the SiO_2 shell.[22] When the aptamer was linked to SiO_2@AuNPs by the Au–S bond, the characteristic absorption peaks of DNA and SiO_2@AuNPs were both found on curve e.

As shown in Fig. 2D, the fluorescence emission of CdS QDs was at 517 nm, and the absorption peak of AuNPs was at 520 nm. Since there was an overlap between the absorption spectra of AuNPs and fluorescence emission spectra of CdS QDs, the ERET could take place between CdS QDs and AuNPs when the distance was in agreement.

3.2 Electrochemical and ECL responses of the modified electrode

The ECL biosensor was characterized by CV and EIS during the preparation process. As shown in Fig. 3, compared to the bare GCE (curve a), the MIL-53(Al) modified electrode (curve b) showed larger current and smaller impedance due to the good electrical conductivity of MIL-53(Al). When the GCE was modified with MIL-53(Al)@CdS-PEI (curve c), the current became larger and the impedance became smaller due to the excellent electron transport of CdS QDs. When CS was incubated on the MIL-53(Al)@CdS-PEI modified electrode, the conductivity was weakened (curve d), because CS is a poor conductive biomacromolecule which hinders the electron transfer. According to the base complementary pairing principle, when the electrode was modified by a SiO_2@AuNPs-aptamer (curve e), the current became larger and the impedance became smaller due to the excellent conductivity of AuNPs.

The ECL performance of the biosensor is shown in Fig. 4. Due to the excellent optical properties of CdS QDs, the ECL

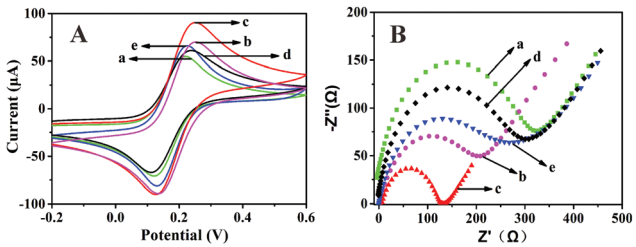

Fig. 3 (A) CVs and (B) EIS Nyquist characterization of the modified electrodes: (a) GCE, (b) GCE/MIL-53(Al), (c) GCE/MIL-53(Al)@CdS-PEI, (d) GCE/MIL-53(Al)@CdS-PEI/CS and (e) GCE/MIL-53(Al)@CdS-PEI/CS/SiO_2@AuNPs-aptamer. CV detection was carried out in a solution containing 0.1 M KCl and 5 mM $K_3Fe(CN)_6$ and EIS Nyquist was detected in a solution containing 5 mM $K_3Fe(CN)_6$/$K_4Fe(CN)_6$ (1 : 1) and 0.1 M KCl.

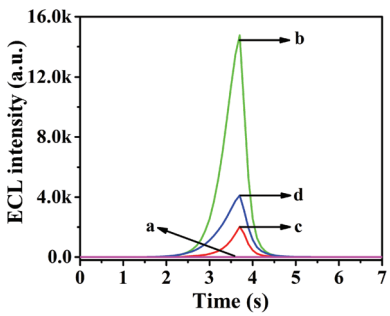

Fig. 4 ECL–time curve of the modified electrode: (a) GCE, (b) MIL-53(Al)@CdS-PEI, (c) MIL-53(Al)@CdS-PEI/CS/SiO_2@AuNPs-aptamer and (d) MIL-53(Al)@CdS-PEI/CS/SiO_2@AuNPs-aptamer/trichlorfon.

This journal is © The Royal Society of Chemistry 2021

Published on 09 December 2020. Downloaded by University of Prince Edward Island on 5/15/2021 6:49:00 AM.

intensity was significantly enhanced when MIL-53(Al)@CdS-PEI (curve b) was modified on the GCE (curve a). When the SiO_2@AuNPs-aptamer (curve c) was incubated on the electrode, which was modified with MIL-53(Al)@CdS-PEI/CS, the ECL intensity was quenched because of the ERET effect on CdS QDs and AuNPs. AuNPs were enriched by SiO_2, which enhanced the ERET interaction and led to the significant weakening of the ECL signal. As shown in curve d, when trichlorfon was present, the binding strength between the aptamer and trichlorfon was greater than the base complementary pairing, so SiO_2@AuNPs-aptamer was dragged away from the surface of the electrode by trichlorfon. As a result, the ERET interaction was weakened and the ECL signal was recovered.

3.3 Optimization of experimental parameters

The ECL intensity was significantly affected by the amount of MIL-53(Al)@CdS-PEI. Owing to the excellent quantum yield of CdS QDs, when the amount of MIL-53(Al)@CdS-PEI increased from 2 μL to 4 μL, the ECL intensity increased (Fig. 5A). But when the amount was larger than 4 μL, the ECL signal gradually decreased, because the excess MIL-53(Al)@CdS-PEI formed a thick film on the electrode, which blocked the transfer of the electrons and ground/excited state transitions of CdS QDs. Therefore, 4.0 μL of MIL-53(Al)@CdS-PEI was chosen for the aptasensor preparation.

To achieve signal amplification, AuNPs were enriched with SiO_2 to synthesize SiO_2@AuNPs. For SiO_2@AuNP fabrication, as described in section 2.4, the amount of AuNPs affected the ECL intensity because AuNPs interacted with CdS QDs that caused the ERET effect to quench the ECL intensity (Fig. 5B). When the mass ratio of AuNPs to SiO_2NPs was less than 0.18, the ECL intensity decreased as the ratio of AuNP increased. The mass ratio of AuNPs to SiO_2NPs reached 0.18, and the ECL intensity was the largest quenched and the ECL signal was the lowest. When the mass ratio of AuNPs to SiO_2NPs was higher than 0.18, too many AuNPs were enriched on the surface of SiO_2 leading to the distance between some AuNPs and CdS QDs becoming greater than 10 nm, thus a SPR effect was generated and the ECL intensity was less quenched. Consequently, the selected mass ratio of AuNPs to SiO_2NPs for the preparation of the SiO_2@AuNP composite was 0.18.

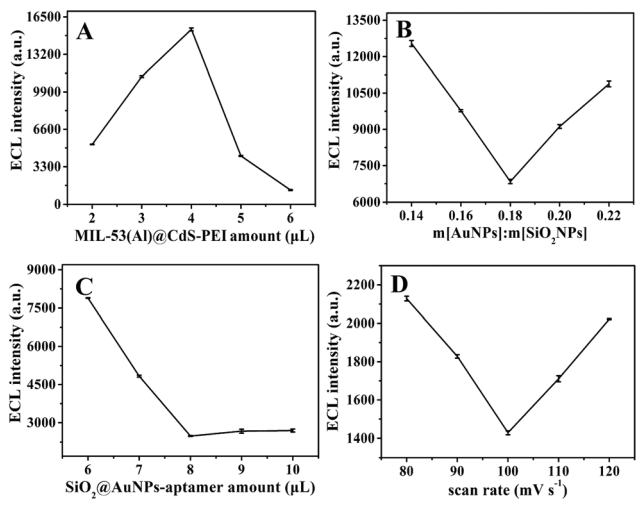

Fig. 5 These factors affected the ECL intensity: (A) the amount of MIL-53(Al)@CdS-PEI, (B) the mass ratio of AuNPs to SiO_2NPs, (C) the amount of SiO_2@AuNPs and (D) the scan rate. Error bar shows the standard deviation of ECL detection performed 3 times.

This experiment investigated the effect of SiO_2@AuNPs-aptamer amount on ECL intensity (Fig. 5C). As the amount of SiO_2@AuNPs-aptamer increased from 6 μL to 8 μL, the ECL intensity decreased, and the lowest intensity was observed at 8 μL. However, when the amount was over 8 μL, the ECL intensity showed a slight change due to the limited base complementary pairing sites on the modified electrode. For the saving reagent, 8 μL was selected as the amount of SiO_2@AuNPs-aptamer.

To obtain the best detection efficiency of the MIL-53(Al)@CdS-PEI modified electrode, the scan rate was studied (Fig. 5D). When the scan rate was increased from 80 mV s^{-1} to 100 mV s^{-1}, the ECL intensity was gradually decreased and reached the lowest quenching at 100 mV s^{-1}; if the scan rate continued to increase, the ECL signal gradually increased. It confirmed that the emitted electrons slowly tend to be saturated at a higher scan rate. Therefore, the conventional scan rate was selected as 100 mV s^{-1}.

3.4 Mechanism of the ECL system

In this system, CdS QDs were used as an emitter and $K_2S_2O_8$ was used as co-reactant, and the possible ECL mechanism is listed as follows:

$$CdS + e^- \rightarrow CdS^{-\bullet}, \quad (1)$$

$$S_2O_8^{2-} + e^- \rightarrow SO_4^{2-} + SO_4^{-\bullet}, \quad (2)$$

$$CdS^{-\bullet} + SO_4^{-\bullet} \rightarrow CdS* + SO_4^{2-}, \quad (3)$$

$$CdS* \rightarrow h\nu + CdS. \quad (4)$$

In Scheme 1, the ECL intensity of MIL-53(Al)@CdS-PEI bound CS with BSA blocked was recorded as ECL-1. Then, the ECL intensity of the SiO_2@AuNPs-aptamer modified electrode was recorded as ECL-2. The intensity of ECL-2 was weaker than that of ECL-1 due to the ERET interaction between AuNPs and CdS QDs, which resulted in the ECL quenching in the process of ECL-2; the excitation energy of CdS QDs was absorbed by the AuNPs, and then the amount of CdS* decreased and the ECL intensity was weakened (the process of eqn (3) was weakened).[23] During the detection of trichlorfon, SiO_2@AuNPs-aptamer was bound to trichlorfon and detached from the modified electrode; the ECL signal was restored (ECL-3) due to the weakened ERET effect.

3.5 Analytical performance of the ECL aptasensor

Under the optimal conditions, the proposed aptasensor was used to detect different concentrations of trichlorfon (Fig. 6). In the range of 10^{-11}–10^{-4} M, the change in the ECL intensity

Published on 09 December 2020. Downloaded by University of Prince Edward Island on 5/15/2021 6:49:00 AM.

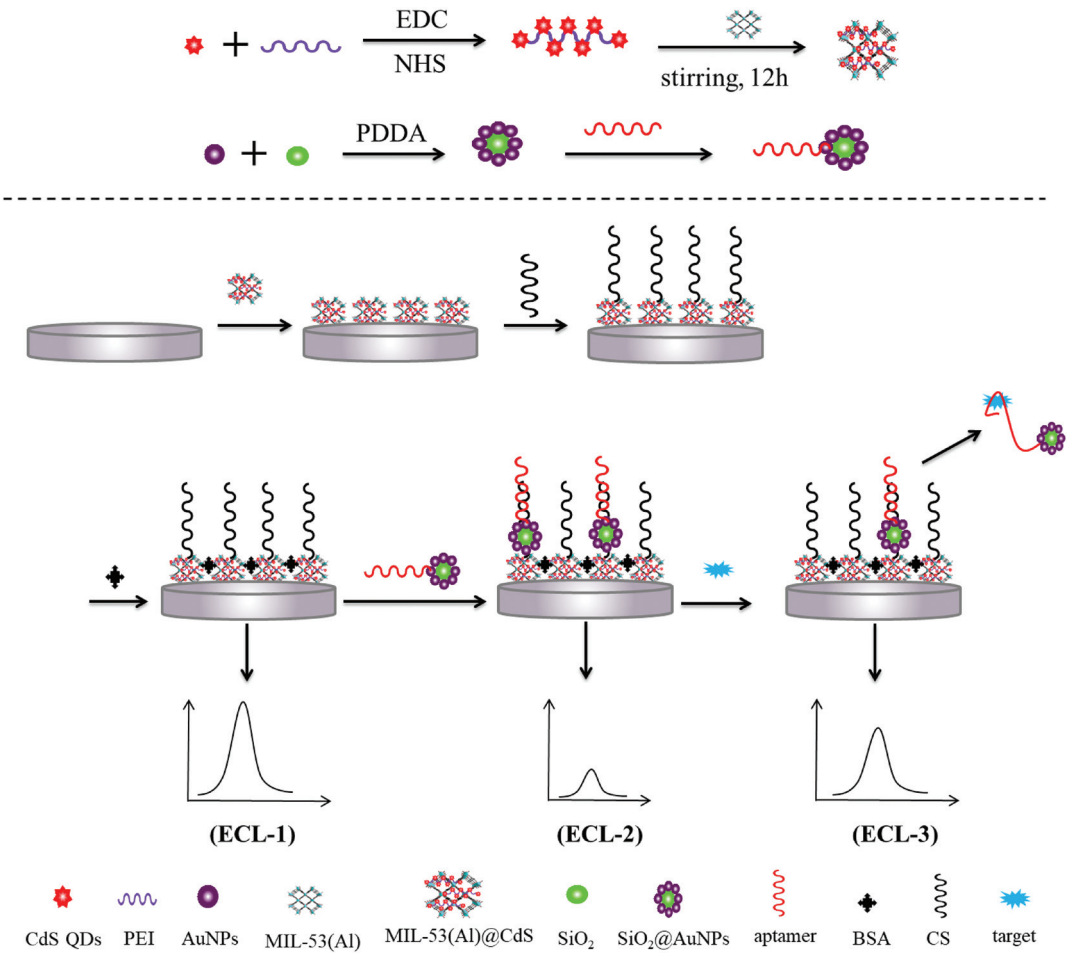

Scheme 1 Schematic of ECL aptasensor fabrication for trichlorfon detection.

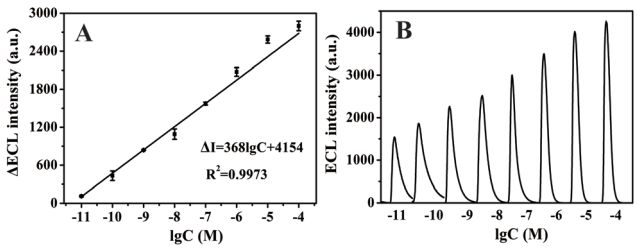

Fig. 6 (A) Plot of Δ*I versus* logarithmic trichlorfon concentrations, and (B) the ECL emission of different concentrations of trichlorfon.

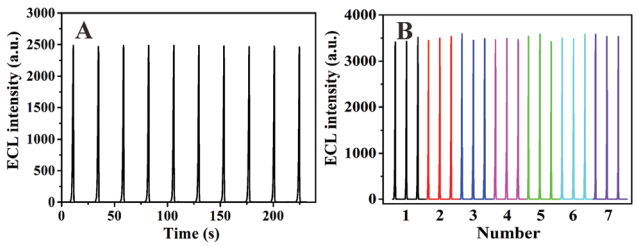

Fig. 7 (A) ECL emission scanned by 10 continuous cycles and (B) the ECL emission of seven different electrodes constructed by the same procedure.

(Δ*I*) presented a linear relationship with the logarithmic concentration of trichlorfon ($\Delta I = 368 \times \lg C + 4154$, $R^2 = 0.9973$), and the detection limit was 5.1×10^{-12} M (S/N = 3, Loock's standard method II[24]).

To evaluate the stability, the aptasensor was tested by consecutive scans for 10 cycles in 10^{-8} M trichlorfon (Fig. 7A), and the aptasensor presented a small relative standard deviation (RSD) of 0.24%. Besides, the aptasensor was placed at 4 °C for 7 days and then assessed by determination 10^{-6} M trichlorfon standard solution; the ECL intensity presented 94.57 ± 2.45% of the original value. The ECL intensity (10^{-6} M trichlorfon) of seven different electrodes prepared by the same procedures was stable with a RSD of 2.50% (Fig. 7B). These experimental results showed that the prepared aptasensor showed excellent repeatability, reproducibility, and stability.

As shown in Fig. 8A, the interference of other organophosphorus pesticides (triazophos, phoxim, methyl parathion, and chlorpyrifos) at the same concentration was investigated. The results indicated that these pesticides exhibited a weak

 This journal is © The Royal Society of Chemistry 2021

Published on 09 December 2020. Downloaded by University of Prince Edward Island on 5/15/2021 6:49:00 AM.

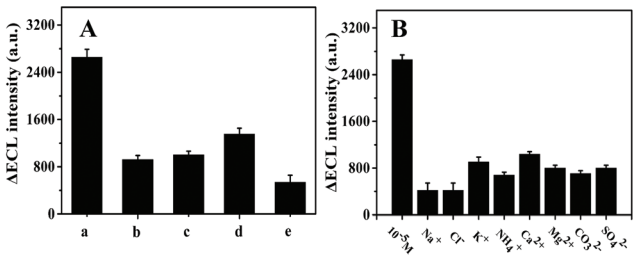

Fig. 8 (A) Selective tests of the ECL aptasensor for the detection of: (a) trichlorfon, (b) triazophos, (c) phoxim, (d) methyl parathion and (e) chlorpyrifos at a concentration of 1.0×10^{-5} M, and (B) the tests for the interference of various ions.

response to the ECL aptasensor. At the same time, the interference of various ions on the aptasensor was also explored. It was found that 10^{-2} M Na^+, Cl^-, K^+, NH_4^+, and 5.0×10^{-2} M Ca^{2+}, Mg^{2+}, CO_3^{2-}, SO_4^{2-} show weak effects on the aptasensor. These results demonstrated that the aptasensor exhibited some selectivity towards organophosphorus pesticides and good anti-interference towards many ions for the determination of trichlorfon.

3.6 Comparison with other methods for trichlorfon detection

The performance of the developed ECL aptasensor is compared with other methods for trichlorfon analysis (Table 1). We found that this aptasensor displayed a wider linear range and lower detection limit, which were better than those displayed by other methods.

3.7 Analysis of food samples

The aptasensor was applied to determine trichlorfon in vegetable samples. In the original samples, no trichlorfon was detected. The obtained recoveries of trichlorfon in lettuce, broccoli, cucumber, and chives samples were 97–105%, 102–104%, 100–104%, and 98–104%, respectively (Table 2). These good results implied that the aptasensor can be successfully used for the detection of trichlorfon in vegetable samples.

Table 1 Performance comparison with other methods for trichlorfon detection

Method	Linear range (M)	Detection limit (M)	Ref.
HPLC	3.9×10^{-8}–3.9×10^{-6}	1.9×10^{-7}	3
GC	2.5×10^{-8}–7.5×10^{-5}	3.5×10^{-8}	4
CE	3.9×10^{-10}–3.9×10^{-5}	5.0×10^{-10}	5
Electrochemical	1.9×10^{-10}–3.5×10^{-8}	1.4×10^{-10}	6
Electrochemical	3.8×10^{-10}–3.8×10^{-8}	3.9×10^{-9}	7
ECL	1.0×10^{-11}–1.0×10^{-4}	5.1×10^{-12}	This work

Table 2 Analytical results obtained for determining trichlorfon in vegetables

Sample	Blank value	Added (M)	Detected (M)	Recovery (%)
Lettuce	Not detected	1.00×10^{-6}	$(1.01 \pm 0.04) \times 10^{-6}$	101± 4
Broccoli	Not detected	1.00×10^{-6}	$(1.03 \pm 0.01) \times 10^{-6}$	103 ± 1
Cucumber	Not detected	1.00×10^{-6}	$(1.02 \pm 0.02) \times 10^{-6}$	102 ± 2
Chives	Not detected	1.00×10^{-6}	$(1.01 \pm 0.03) \times 10^{-6}$	101 ± 3

4 Conclusions

In conclusion, we reported a signal amplified electrochemiluminescence sensor based on MIL-53(Al)@CdS-PEI and SiO_2@AuNPs for trichlorfon detection. The proposed aptasensor presented good analytical performance including a lower detection limit, a wider linear range, and excellent selectivity, reproducibility, and stability. The ECL aptasensor was successfully applied to determine trichlorfon in vegetable samples with satisfying results. Thus, this study proposed a new potential method for detecting trichlorfon.

Conflicts of interest

There are no conflicts to declare.

Acknowledgements

The project was supported by the National Natural Science Foundation of China (No. 21365004), the Guangxi Natural Science Foundation (No. 2018GXNSFAA138086), the Key Research and Development Project of Guangxi (AB18126048), the Specific Research Project of Guangxi for Research Bases and Talents (AD18126005), and the Shandong Key Laboratory of Biochemical Analysis (SKLBA1910).

Notes and references

1 N. Gao, C. He, M. Ma, Z. Cai, Y. Zhou, G. Chang, X. Wang and Y. He, *Anal. Chim. Acta*, 2019, **1072**, 25–34.
2 T. H. V. Kumar and A. K. Sundramoorthy, *Anal. Chim. Acta*, 2019, **1074**, 131–141.
3 M. Xue, J. Shen, D. Wang, L. Yin, X. Zhuang and Z. Meng, *Anal. Methods*, 2015, **7**, 2420–2424.
4 Q. Liu, M. Jiang, Z. Ju, X. Qiao and Z. Xu, *Food Chem.*, 2018, **250**, 134–139.
5 J. Li, J. Lu, X. Qiao and Z. Xu, *Food Chem.*, 2017, **221**, 1285–1290.
6 H. Dzudzevic-Cancar, S. Soylemez, Y. Akpinar, M. Kesik, S. Goker, G. Gunbas, M. Volkan and L. Toppare, *ACS Appl. Mater. Interfaces*, 2016, **8**, 8058–8067.
7 P. Zhang, T. Sun, S. Rong, D. Zeng, H. Yu, Z. Zhang, D. Chang and H. Pan, *Bioelectrochemistry*, 2019, **127**, 163–170.
8 M. M. Richter, *Chem. Rev.*, 2004, **104**, 3003–3036.
9 X. Li, X. Tan, J. Yan, Q. Hu, J. Wu, H. Zhang and X. Chen, *Electrochim. Acta*, 2016, **187**, 433–441.

Published on 09 December 2020. Downloaded by University of Prince Edward Island on 5/15/2021 6:49:00 AM.

10 X. Zhong, X. Li, Y. Zhuo, Y. Chai and R. Yuan, *Sens. Actuators, B*, 2020, **305**, 127490.
11 D. Feng, X. Tan, Y. Wu, C. Ai, Y. Luo, Q. Chen and H. Han, *Biosens. Bioelectron.*, 2019, **129**, 100–106.
12 F. Yang, X. Zhong, X. Jiang, Y. Zhuo, R. Yuan and S. Wei, *Biosens. Bioelectron.*, 2019, **130**, 262–268.
13 X. Huang, Y. Zhang, W. Xu, W. Xu, L. Guo, B. Qiu and Z. Lin, *Chem. Commun.*, 2019, **55**, 12980–12983.
14 T. Neumann, M. L. Johansson, D. Kambhampati and W. Knoll, *Adv. Funct. Mater.*, 2002, **12**, 575–586.
15 B. Babamiri, A. Salimi and R. Hallaj, *Biosens. Bioelectron.*, 2018, **102**, 328–335.
16 S. Chen, X. Chen, T. Xia and Q. Ma, *Biosens. Bioelectron.*, 2016, **85**, 903–908.
17 S. L. James, *Chem. Soc. Rev.*, 2003, **32**, 276.
18 P. Falcaro, R. Ricco, C. M. Doherty, K. Liang, A. J. Hill and M. J. Styles, *Chem. Soc. Rev.*, 2014, **43**, 5513–5560.
19 T. Loiseau, C. Serre, C. Huguenard, G. Fink, F. Taulelle, M. Henry, T. Bataille and G. Ferey, *Chemistry*, 2004, **10**, 1373–1382.
20 G. C. Fan, H. Zhu, Q. Shen, L. Han, M. Zhao, J. R. Zhang and J. J. Zhu, *Chem. Commun.*, 2015, **51**, 7023–7026.
21 L. Meng, X. Qiao, J. Song, Z. Xu, J. Xin and Y. Zhang, *J. Agric. Food Chem.*, 2011, **59**, 12745–12751.
22 C. Wang, Z. Ma, T. Wang and Z. Su, *Adv. Funct. Mater.*, 2006, **16**, 1673–1678.
23 Y. Shan, J. J. Xu and H. Y. Chen, *Chem. Commun.*, 2009, 905–907.
24 H. P. Loock and P. D. Wentzell, *Sens. Actuators, B*, 2012, **173**, 157–163.

This journal is © The Royal Society of Chemistry 2021